Korean J. Chem. Eng., **22**(5), 793-796 (2005)

Submicron Patterning of Ta, NiFe, and Pac-man Type Ta/NiFe/Ta Magnetic Elements

Hyun-Wook Ra, Kwang Sup Song* and Yoon-Bong Hahn†

School of Chemical Engineering and Technology, Nanomaterials Processing Research Center,
Chonbuk National University, Chonju 561-756, Korea
*Korea Institute of Energy Research, Daejeon 305-343, Korea
(*Received 10 March 2005 • accepted 30 May 2005*)

Abstract−Submicron patterning of Ta, NiFe, and Pac-man type magnetic elements of Ta/NiFe/Ta has been carried out in inductively coupled plasmas (ICPs) of Cl_2/Ar. Etch behavior was quite dependent on materials and plasma parameters. An ion-enhanced etch mechanism played a critical role for desorption of metal chloride etch products. Sidewall contamination with etch products was observed at a higher Cl_2 concentration (>50%). Compared to relatively damaged surfaces and profiles by the ion milling method, the ICP etching technique produced clear, smooth, and well-defined Pac-man type elements.

Key words: Magnetic Elements, Submicron Patterning, Dry Etching, Pac-man Type

INTRODUCTION

Magnetic random access memory (MRAM) devices have attracted much attention for the last few years due to their great potential as commercial devices such as nonvolatility, high speed, low power consumption, thermal stability, and unlimited read/write operations [Tsang, 1991; Jung et al., 1999; Cho et al., 2002]. Most magnetic elements for the MRAM devices have been linear in shape with modified ends such as a hexagon or an ellipse, not only because of simple patterning, but also fewer magnetic defects. However, edge domains of an array of magnetic submicron elements are very sensitive to the small end shape variation between elements and edge roughness caused by limited lithographic resolution [Portier and Petford-Long, 2000; Zheng and Zhu, 1997; Fang and Zhu, 2000; Park et al., 2003]. This leads to significant variations in the magnetic switching field. To enhance the switching behavior of submicron magnetic elements, a Pac-man type element was first proposed by Park et al. [2003] They reported a significant improvement for the future magnetic element design of the MRAM devices.

To increase the storage densities of the MRAM, the structures of the MRAM device also need to be downscaled. This requires new processes for patterning of magnetic materials, as currently applied methods like ion milling [Gokan and Esho, 1981] and reactive ion etch (RIE) [Vasile and Mogab, 1986] cannot provide the required etch profile and etch rates. The problem with dry etching of magnetic materials is the low volatility of the etch products. This means that etch rates are too slow to be commercially viable. Therefore, a good alternative is the high density plasma etching which can provide the required anisotropic process and relatively high etch rate for magnetic materials due to the efficient desorption of etch products by high ion fluxes [Jung et al., 1999; Cho et al., 2000; Hahn and Pearton, 2000; Park et al., 2004; Ra et al., 2005].

In this paper, we report on sub-micron etch characteristics of Ta, NiFe, and Ta/NiFe/Ta with Cl_2/Ar inductively coupled plasmas for MRAM applications. We investigated etch rate and etch profile as a function of the processing parameters such as operating pressure, rf chuck power, ICP source power, and etch gas concentration. Especially, we patterned a submicron Pac-man type elements of Ta/NiFe/Ta and compared the attained etch profile with the configuration obtained by ion-milling method. The ICP etching technique produced a better profile than the ion-milling method.

EXPERIMENTS

Thin films of NiFe (300 nm), Ta (300 nm), and Ta (5 nm)/NiFe (5 nm)/Ta (5 nm) were deposited on top of silicon (100) wafers by a rf magnetron sputtering from composite targets. The magnetic films were coated with a 200 nm thick layer of the negative type Ma-N-2403 photoresist (Micro Chem.). The Pac-man type elements of Ta/NiFe/Ta were patterned by using electron-beam lithography and ion milling and ICP etching methods. The photoresist was removed after etching and the samples were rinsed in de-ionized water to remove the chloride etch products [Park et al., 2004]. The etch depths of the etched samples were measured by stylus profilometry, while the etch profiles were examined by scanning electron microscope (SEM).

The dry etching was performed in a planar type ICP system (Vacuum Science ICP etcher, VSICP-1250A), with the samples placed on an rf powered (13.56 MHz) helium backside-cooled electrode. The operating pressure was varied from 5 to 20 mTorr. The rf chuck power was varied from 100 W to 250 W, while the ICP source power was varied from 600 W to 1,000 W. A Cl_2/Ar mixture, with total gas flow rate of 20 standard cubic centimeters per minute (sccm), was injected into the ICP etcher through mass flow controllers.

RESULTS AND DISCUSSION

The operating pressure affects the etch rates of the magnetic films and dc bias voltage as shown in Fig. 1. The operating pressure was varied from 5 to 20 mTorr at 700 W ICP source power, 150 W rf chuck power, and 25% Cl_2 concentration. NiFe showed a maximum

---

[†] To whom correspondence should be addressed.
E-mail: ybhahn@chonbuk.ac.kr

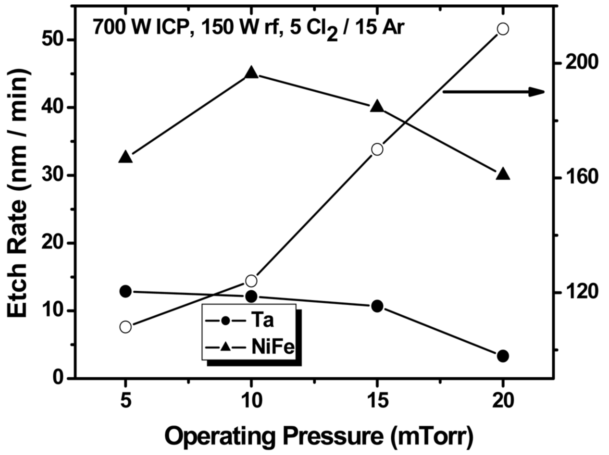

Fig. 1. Effect of operating pressure on etch rate and dc bias voltage at 700 W ICP, 150 W rf, and 25% Cl_2.

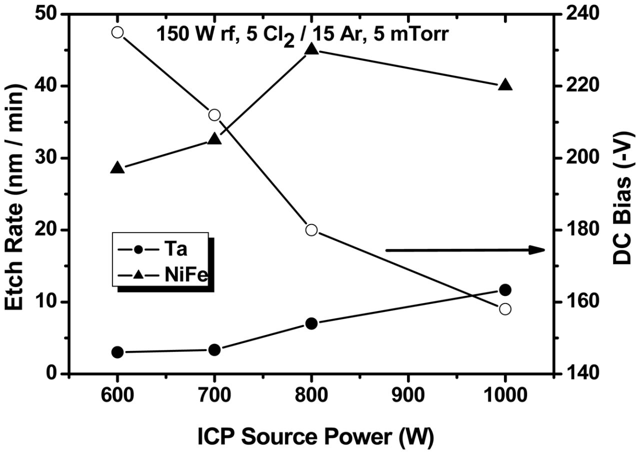

Fig. 3. Effect of ICP source power on etch rate and dc bias voltage at 150 W rf, 25% Cl_2, and 5 mTorr.

etch rate at 10 mTorr. However, the etch rate of Ta decreased gradually with increasing the operating pressure. In general, the concentration of neutrals increases with increasing the pressure, but at the same time the recombination rate of ions and electrons in the plasma also increases with pressure [Liberman and Lichtenberg, 1994]. The increase in recombination rate then produces fewer incident ions onto the sample surfaces, resulting in less effect of physical sputtering on removal of etch products. Hence, the etch rate of magnetic films decreased at a higher operating pressure mainly due to the more recombination of ions and shorter mean free path of ions.

Fig. 2 clearly shows the effect of the rf chuck power on the etch rate and dc bias voltage at constant source power, Cl_2 concentration, and operating pressure. The main role of the chuck power is to increase the ion-bombarding energy. The etch rate of NiFe and the dc bias voltage increased with the rf chuck power. The increase in etch rate with the chuck power is explained by enhanced sputter desorption of etch products as the ion energy increases. However, the decrease in the etch rate of Ta at a higher rf chuck power (>200 W) is attributed to the desorption of adsorbed chlorine neutrals by increased ion energy before they do react with the sample surface [Im et al., 2001; Park et al., 2003].

The ICP source power controls the ion flux incident on the sample surface. Fig. 3 shows the effect of ICP source power on the etch rate and dc bias voltage. During these experiments, the rf chuck power, Cl_2 concentration, and operating pressure were kept constant at 150 W, 25%, and 5 mTorr, respectively. Ta and NiFe showed a gradual increase in the etch rate with increasing the ICP source power. In general, a greater ion flux is obtained at a higher ICP source power. The increase in etch rate with the ICP source power is thus attributed to an ion-enhanced etch mechanism, indicating that the ion-enhanced etch took a critical role for desorption of the chlorine etch products.

Fig. 4 presents the effect of Cl_2 concentration on the etch rate and dc bias voltage. The etch rates were very slow when pure Ar or Cl_2 was used, indicating that the etch rate is mainly due to physical sputtering with only Ar, whereas it is attributed to the chemical etch component with pure Cl_2. However, when both were used, the etch rates became much greater than the sum of individual rates. This implies that the modification of the substrate surface by bombarding ions which significantly enhances the rate of gas-solid reaction

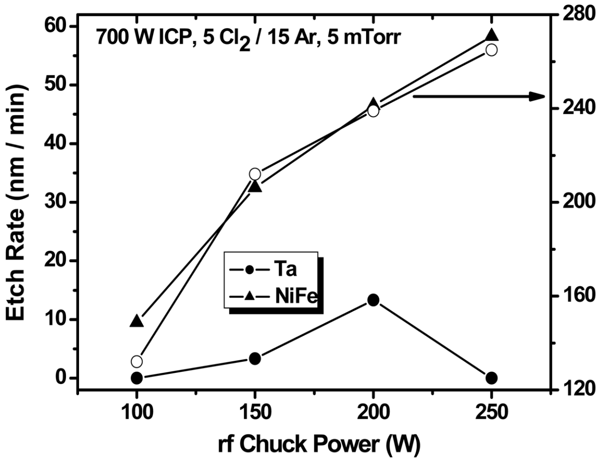

Fig. 2. Effect of rf chuck power on etch rate and dc bias voltage at 700 W ICP, 25% Cl_2, and 5 mTorr.

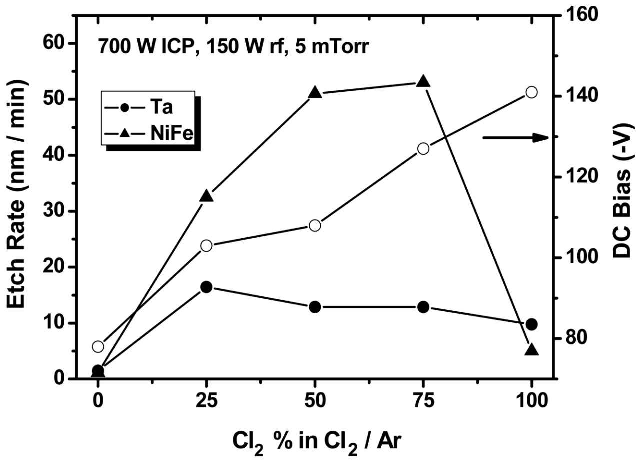

Fig. 4. Effect of Cl_2 concentration on etch rate and dc bias voltage at 700 W ICP, 150 W rf, and 5 mTorr.

is more important than the nature of the reactive species generated in plasma. The etch rate of NiFe achieved a maximum value at 75% Cl_2 concentration, but that of Ta decreased with the Cl_2 concentration, which is a behavior observed frequently for the materials producing relatively low-volatility etch products. The dc bias voltage increased with increasing the Cl_2 concentration. This may be explained by the fact that compared to pure Ar discharges, additional collisional energy losses are present with increasing the Cl_2 concentration, resulting in less production of ions [Ra et al., 2004]. The lower ion flux at a higher Cl_2 percentage (>75%) thus explains in part the lower etch rates with high chlorine content.

The etched features of magnetic films were examined by using SEM. Fig. 5 shows the SEM micrographs of the Pac-man type elements of Ta/NiFe/Ta obtained by ion milling (a) and Cl_2/Ar ICP etching (b), respectively. Compared to the clear, smooth and well-defined pattern by the ICP etching technique, the ion milling method produced relatively damaged surfaces and profiles mainly due to the higher ion energy. In this work, it was found that the etch pro-

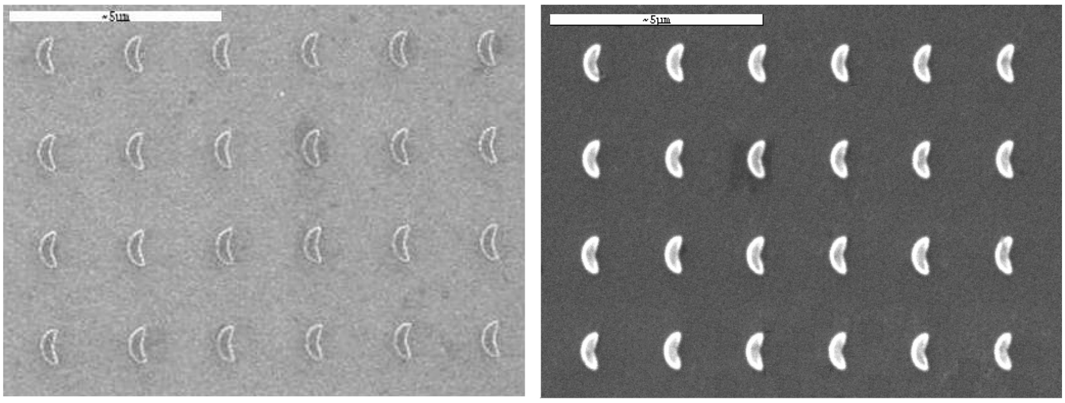

(a) Ion milling (b) Cl_2/Ar ICP etching

Fig. 5. SEM images of Pac-man type elements of Ta/NiFe/Ta patterned by ion milling (a) and Cl_2/Ar ICP etching (b).

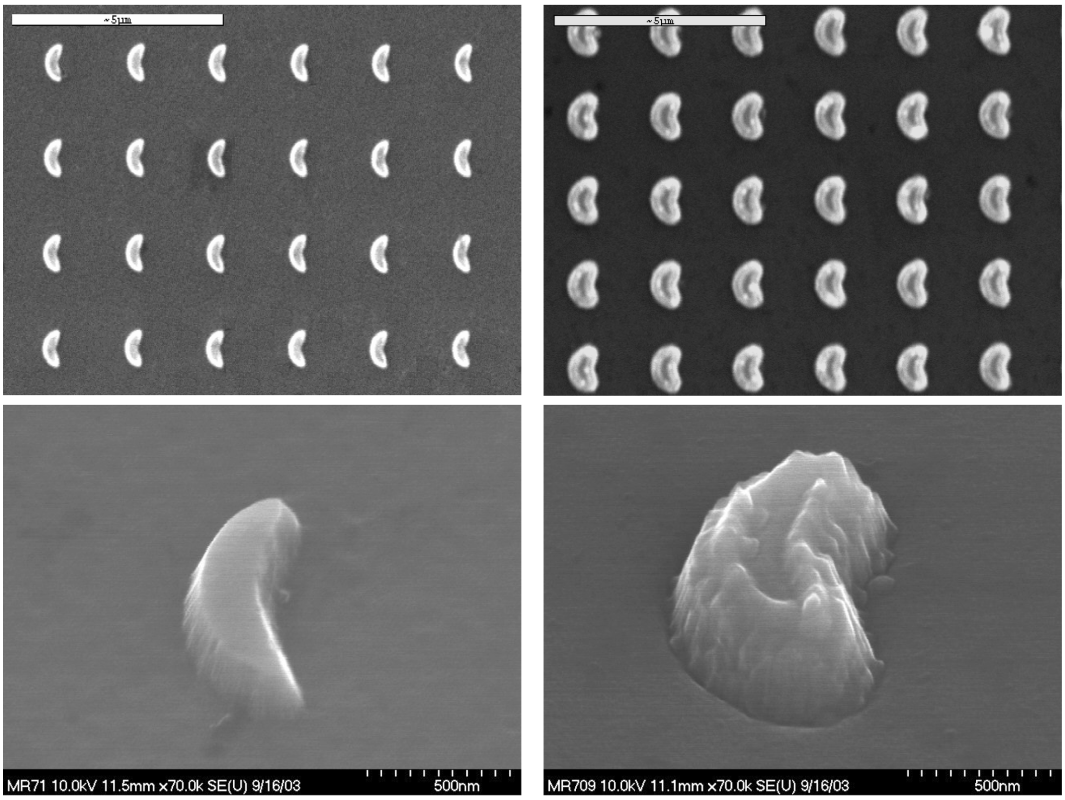

(a) 10 % Cl_2 (b) 50 % Cl_2

Fig. 6. Low (top) and high (bottom) magnification SEM images of Pac-man type elements of Ta/NiFe/Ta etched with (a) 10% and (b) 50% Cl_2 at 700 W ICP, 150 W rf, and 5 mTorr.

file of Ta/NiFe/Ta multilayer is quite dependent on the concentration of Cl_2. Fig. 6 shows the low and high magnification SEM images of the Pac-man type permalloy element etched with two different Cl_2 concentrations of 10% (a) and 50% (b), respectively, at 700 W ICP source power, 150 W rf chuck power, and 5 mTorr pressure. The micrographs show quite smooth surface, clean sidewall, contamination free, and anisotropic profile with 10% Cl_2, while the sidewall is contaminated with deposition of etch products with 50% Cl_2. In conclusion, the results obtained from this work indicate that the ICP etching with Cl_2/Ar discharges can be utilized for submicron pattern transfer of the magnetic elements for MRAM devices.

CONCLUSIONS

High density plasma etching of NiFe, Ta, and Pac-man type elements of Ta/NiFe/Ta was carried out with Cl_2/Ar discharges. NiFe showed a maximum etch rate at an operating pressure of 10 mTorr while the etch rate of Ta decreased with increasing the pressure. The etch rate of NiFe and the dc bias voltage increased with the rf chuck power. Ta showed a gradual increase in the etch rate with increasing the ICP source power, while the NiFe showed a maximum etch rate (45 nm/min) at 800 W ICP source power. The etch rate of NiFe achieved a maximum value at 75% Cl_2 concentration, but that of Ta decreased with Cl_2 concentration. Compared to relatively damaged surfaces and profiles by the ion milling method, the ICP etching technique produced clear, smooth, contamination free, and well-defined Pac-man type elements.

ACKNOWLEDGMENTS

This paper was supported in part by research funds of Chonbuk National University and by the NRL program through Korea Institute of Energy Research.

REREFENCES

Cho, H. G., Kim, Y. K. and Lee, S. R., “Magnetic and Magnetoresistance Properties of Synthetic Spin Valves with Different Pinning Layer Thicknesses,” *J. Korean Phys. Soc.*, **41**, 753 (2002).

Cho, H., Lee, K.-P., Jung, K. B., Pearton, S. J., Marburger, J., Sharifi, F., Hahn, Y. B. and Childress, J. R., “Corrosion-free Dry Etch Patterning of Magnetic Random Access Memory Stacks: Effects of Ultraviolet Illumination,” *J. Appl. Phys.*, **87**, 6397 (2000).

Fang, T. N. and Zhu, J. G., “Switching Fluctuations and Density Limitations of Pseudospin Valve Memory,” *J. Appl. Phys.*, **87**, 7061 (2000).

Gokan, H. and Esho, S., “Pattern Fabrication by Oblique Incidence Ion-beam Etching,” *J. Vac. Sci. Technol.*, **18**, 23 (1981).

Hahn, Y. B., Hays, D. C., Cho, H., Jung, K. B., Abernathy, C. R., Donovan, S. M., Pearton, S. J., Han, J. and Shul, R. J., “Comparison of ICl- and IBr-based Plasma Chemistries for Inductively Coupled Plasma Etching of GaN, InN and AlN,” *Mater. Sci. Eng.*, **B60**, 95 (1999).

Hahn, Y. B., Hays, D. C., Cho, H., Jung, K. B., Abernathy, C. R. and Pearton, S. J., “Effect of Inert Gas Additive Species on Cl_2 High Density Plasma Etching of Compound Semiconductors: Part I. GaAs and GaSb,” *Appl. Surf. Sci.*, **147**, 207 (1999).

Hahn, Y. B. and Pearton, S. J., “A Unified Global Self-Consistent Model of a Capacitively and Inductively Coupled Plasma Etching System,” *Korean J. Chem. Eng.*, **17**, 304 (2000).

Im, Y. H., Choi, C. S. and Hahn, Y. B., “High Density Plasma Etching of GaN Films in Cl_2/Ar Discharges with a Low-Frequency-Excited DC Bias,” *J. Korean Phys. Soc.*, **39**, 617 (2001).

Jung, K. B., Cho, H., Hahn, Y. B., Hays, D. C., Lambers, E. S., Park, Y. D., Feng, T., Childress, J. R. and Pearton, S. J., “Effect of Inert Gas Additive on Cl_2-based Inductively Coupled Plasma Etching of NiFe and NiFeCo,” *J. Vac. Sci. Technol. A*, **17**, 2223 (1999).

Jung, K. B., Cho, H., Hahn, Y. B., Hays, D. C., Lambers, E. S., Park, Y. D., Feng, T., Childress, J. R. and Pearton, S. J., “Effect of Inert Gas Additive on Cl_2-based Inductively Coupled Plasma Etching of NiFe and NiFeCo,” *J. Vac. Sci. Technol. A*, **17**, 2223 (1999).

Jung, K. B., Cho, H., Hahn, Y. B., Hays, D. C., Lambers, E. S., Park, Y. D., Feng, T., Childress, J. R. and Pearton, S. J., “Relative Merits of Cl_2 and CO/NH_3 Plasma Chemistries for Dry Etching of Magnetic Random Access Memory Device Elements,” *J. Appl. Phys.*, **85**, 4788 (1999).

Jung, K. B., Cho, H., Hahn, Y. B., Hays, D. C., Lambers, E. S., Park, Y. D., Feng, T., Childress, J. R. and Pearton, S. J., “Interhalogen Plasma Chemistries for Dry Etch Patterning of Ni, Fe, NiFe and NiFeCo Thin Films,” *Appl. Surf. Sci.*, **140**, 215 (1999).

Liberman, M. A. and Lichtenberg, A. J., *Principles of Plasma Discharges and Materials Processing*, John-Wiley and Sons, N. Y. (1994).

Park, H. J., Ra, H.-W., Song, K. S. and Hahn, Y. B., “ Inductively Coupled Plasma Etching of Ta, Co, Fe, NiFe, NiFeCo, and MnNi with Cl_2/Ar Discharges,” *Korean J. Chem. Eng.*, **21**, 1235 (2004).

Park, J. S., Park, H. J., Hahn, Y. B., Yi, G.-C. and Yoshikawa, A., “Dry Etching of ZnO Films and Plasma-induced Damage to Optical Properties,” *J. Vac. Sci. Technol. B*, **21**, 800 (2003).

Park, M. H., Hong, Y. K., Gee, S. H. and Erickson, D. W., “Magnetization Configuration and Switching Behavior of Submicron NiFe Elements: Pac-man Shape,” *Appl. Phys. Lett.*, **83**, 329 (2003).

Portier, X. and Petford-Long, A. K., “The Formation of 360° Domain Walls in Magnetic Tunnel Junction Elements,” *Appl. Phys. Lett.*, **76**, 754 (2000).

Ra, H.-W., Park, H. J., Kim, K. J., Kim, W.-Y. and Hahn, Y.-B., “Dry Etching of NiFe, NiFeCo, and Ta in Cl_2/Ar Inductively Coupled Plasma,” *Korean Chem. Eng. Res.*, **43**, 76 (2005).

Ra, H.-W., Hahn, Y. B., Song, K. S., Park, M. H. and Hong, Y. K., “Dry Etching of NiFe/Co and NiFe/Al-O/Co Multilayers in an Inductively Coupled Plasma of Cl_2/Ar Mixture,” *J. Vac. Sci. Technol. A*, **22**, 2388 (2004).

Tsang, C. H., “Design and Performance Considerations in High Areal Density Longitudinal Recording (Invited),” *J. Appl. Phys.*, **69**, 5393 (1991).

Vartuli, C. B., Pearton, S. J., Lee, J. W., Mackenzie, J. D., Abernathy, C. R., Shul, R. J., Constantine, C. and Barratt, C., “Inductively Coupled Plasma Etching of III-V Nitrides in CH_4/H_2/Ar and $CH_4/H_2/N_2$ Chemistries,” *J. Electrochem. Soc.*, **144**, 2844 (1997).

Vasile, M. J. and Mogab, C. J., “Chemically Assisted Sputter Etching of Permalloy using CO or Cl_2,” *J. Vac. Sci. Technol. A*, **4**, 1841 (1986).

Zheng, Y. and Zhu, J. G., “Switching Field Variation in Patterned Submicron Magnetic Film Elements,” *J. Appl. Phys.*, **81**, 5471 (1997).